HHS Public Access

Author manuscript

Stroke. Author manuscript; available in PMC 2021 March 29.

Published in final edited form as:

Stroke. 2017 September ; 48(9): 2441–2449. doi:10.1161/STROKEAHA.117.017773.

Long-Delay Arterial Spin Labeling Provides More Accurate Cerebral Blood Flow Measurements in Moyamoya Patients:

A Simultaneous Positron Emission Tomography/MRI Study

Audrey P. Fan, PhD, **Jia Guo, PhD**, **Mohammad M. Khalighi, PhD**, **Praveen K. Gulaka, PhD**, **Bin Shen, PhD**, **Jun Hyung Park, PhD**, **Harsh Gandhi, MS**, **Dawn Holley, BS, CNMT**, **Omar Rutledge, MS**, **Prachi Singh, PhD**, **Tom Haywood, PhD**, **Gary K. Steinberg, MD, PhD**, **Frederick T. Chin, PhD**, **Greg Zaharchuk, MD, PhD**

Departments of Radiology (A.P.F., J.G., P.K.G., B.S., J.H.P., H.G., D.H., O.R., P.S., T.H., F.T.C., G.Z.) and Neurosurgery (G.K.S.), Stanford University, CA; and Global Applied Science Lab, GE Healthcare, Menlo Park, CA (M.M.K.).

Abstract

Background and Purpose——Arterial spin labeling (ASL) MRI is a promising, noninvasive technique to image cerebral blood flow (CBF) but is difficult to use in cerebrovascular patients with abnormal, long arterial transit times through collateral pathways. To be clinically adopted, ASL must first be optimized and validated against a reference standard in these challenging patient cases.

Methods——We compared standard-delay ASL (post-label delay=2.025 seconds), multidelay ASL (post-label delay=0.7–3.0 seconds), and long-label long-delay ASL acquisitions (post-label delay=4.0 seconds) against simultaneous [^{15}O]-positron emission tomography (PET) CBF maps in 15 Moyamoya patients on a hybrid PET/MRI scanner. Dynamic susceptibility contrast was performed in each patient to identify areas of mild, moderate, and severe time-to-maximum (Tmax) delays. Relative CBF measurements by each ASL scan in 20 cortical regions were compared with the PET reference standard, and correlations were calculated for areas with moderate and severe Tmax delays.

Results——Standard-delay ASL underestimated relative CBF by 20% in areas of severe Tmax delays, particularly in anterior and middle territories commonly affected by Moyamoya disease (P<0.001). Arterial transit times correction by multidelay acquisitions led to improved consistency with PET, but still underestimated CBF in the presence of long transit delays (P=0.02). Long-label long-delay ASL scans showed the strongest correlation relative to PET, and there was no difference in mean relative CBF between the modalities, even in areas of severe delays.

Conclusions——Post-label delay times of ≥4 seconds are needed and may be combined with multidelay strategies for robust ASL assessment of CBF in Moyamoya disease.

Correspondence to Audrey P. Fan, PhD, Department of Radiology, Stanford University, 1201 Welch Rd, Stanford, CA 94305. auddie@stanford.edu.

Keywords

cerebral blood flow; cerebrovascular circulation; magnetic resonance imaging; Moyamoya disease; positron-emission tomography

Noninvasive assessment of cerebral blood flow (CBF) provides critical information to diagnose and manage therapy for patients with cerebrovascular disorders, including acute stroke and Moyamoya disease. Patients with Moyamoya disease experience progressive stenosis of arteries at the base of the brain, particularly of the anterior circulation, and develop extensive collateral vasculature to compensate.[1] Although some patients experience cerebral ischemia or hemorrhage,[2] others maintain adequate compensatory blood supply through collaterals and remain asymptomatic into adulthood.[3] Thus, it is important to monitor cerebral perfusion status to grade disease severity and identify candidates for surgical treatments that may improve clinical outcomes. Given the central role of cerebrovascular reserve (CVR) measurement (ie, the ability of the brain to augment perfusion in response to a vasodilatory challenge) in the symptomatology and the management of patients with chronic ischemia, validating new imaging methods against a reference standard is of paramount importance.

Positron emission tomography (PET) with [^{15}O]-water radiotracers remains the reference standard for CBF imaging and provides quantitative characterization of hemodynamics in Moyamoya disease[4,5] and patient response to bypass surgery.[6] Unfortunately, [^{15}O]-water PET requires an on-site cyclotron and complex procedures that are prohibitive in most clinical settings. Dynamic susceptibility contrast (DSC) MRI has also been used to evaluate CBF abnormalities[7] and surgical revascularization in Moyamoya disease.[8,9] However, DSC requires administration of an exogeneous tracer, and the input function is difficult to estimate in the presence of long transit delays and dispersion.[8] These effects limit the accuracy of DSC perfusion maps and may confound the interpretation of hemodynamic changes observed after surgery or during a vasodilatory challenge.

Among the most promising noninvasive techniques for perfusion imaging is arterial spin labeling (ASL) MRI that magnetically labels endogenous, flowing spins in feeding arteries to image CBF. ASL has demonstrated potential in numerous cerebrovascular and neurological disorders,[10] leading to a recent multisite effort to standardize the ASL acquisition.[11] However, typical ASL protocols fail in regions with long transit delays through collateral pathways, for example, in Moyamoya patients with abnormally long Tmax (time-to-maximum of the residue function) on DSC.[12,13] In these patients, if the prescribed post-labeling delay (PLD) is too short relative to the arrival time of tagged spins, ASL underestimates or fails to detect blood flow through collateral vasculature.[14] For ASL to accurately measure CBF in Moyamoya disease or other steno-occlusive disorders, more sophisticated acquisitions are necessary.

This study investigates the accuracy of several ASL acquisitions in Moyamoya patients, including standard-delay acquisition, multidelay acquisition with correction for measured arterial transit time (ATT), and long-label long-delay acquisition. We compared ASL measurements against simultaneous reference [^{15}O]-water PET scans on a hybrid PET/MRI

system. The accuracy of relative CBF measurements from ASL with respect to PET was investigated in brain regions of different disease severity as classified by a separate DSC scan.

Materials and Methods

Patient Population

Fifteen patients with Moyamoya disease undergoing evaluation for bypass surgery were recruited for PET/MRI scans (Table 1). Inclusion criteria included age of ≥15 years and a confirmed diagnosis of Moyamoya disease based on either 1 or more of the following diagnostic tests: cerebral angiogram, MRI/magnetic resonance angiography, and computed tomographic angiogram. Exclusion criteria included known allergies to sulfa drugs or contrast agent, impaired renal function that would preclude administration of contrast agent, or any contraindication to MRI. The study was performed in compliance with the Stanford University Institutional Review Board, and all patients provided written informed consent before the study. Participants were requested to refrain from caffeine intake for 6 hours before the study.

PET/MRI Acquisition

All images were acquired on a simultaneous time-of-flight enabled 3.0 Tesla PET/MRI system (Signa, GE Healthcare, Waukesha, WI). For PET-based perfusion scans, each patient received manual, intravenous injection of [^{15}O]-water (490–960 MBq) through an antecubital vein. PET acquisition commenced with the tracer injection, and the first 2 minutes of PET counts after tracer administration were reconstructed to create a map of relative CBF. PET reconstruction was performed with a TOF-OSEM algorithm (time-of-flight ordered subset expectation maximization; 4 iterations and 28 subsets) on a 192×192 matrix, 30 cm field-of view, 2.78 mm slice thickness, and included correction for scatter, random counts, dead time, and point-spread function. During each PET scan, liver-accelerated volume acquisition-Flex 2-point Dixon MRI scans were acquired for attenuation correction with an atlas-based algorithm.[15]

Three ASL MRI scans were performed simultaneously with the [^{15}O]-water PET scan (Table 2). All ASL scans used pseudocontinuous labeling, had a 3-dimensional fast spin echo readout with stack-of-spirals readout trajectory, and were designed with similar scan time of ≈5 minutes. The labeling duration (LD) and PLD times of the standard-delay ASL scan were chosen based on recent consensus values for clinical patients, with LD/PLD of 1.5/2.0 seconds.[11] The multidelay ASL scan consisted of a slightly longer LD duration (2 seconds) and included 5 PLD times between 0.7 and 3.0 seconds, enabling measurement of and correction for ATT. Finally, the long-label long-delay (LLLD) ASL scan had a single, longer PLD of 4 seconds to help ensure arrival of tagged blood, with longer LD (3 seconds) to improve the signal-to-noise ratio. No vascular crushing was applied.

All patients received 3-dimensional T_1-weighted scans with an inversion-recovery prepared, fast spoiled gradient recalled sequence (repetition time=9.5 ms; echo time=3.8 ms; spatial resolution=0.93×0.93×1 mm^3). DSC MRI was performed using 0.1 mmol/kg of gadolinium

contrast injected at 4 mL/s at the end of the study. DSC scan parameters included 60 time points, 19 slices, spatial resolution of 1.875×1.875×5.0 mm^3, repetition time=1800 ms, and echo time=40 ms; and images were processed with RAPID software[16] to create Tmax maps.

ASL Measurements

Perfusion maps from the standard-delay and LLLD ASL scans were generated from a 1-compartment model:

$$CBF = 6000 \cdot \frac{e^{PLD/T_{1a}}}{2\varepsilon T_{1a}\left(1 - e^{-LD/T_{1a}}\right)} \cdot \lambda \cdot \frac{M}{M_0} \quad (1)$$

where ΔM represents the perfusion difference signal, and M_0 represents the fully relaxed, equilibrium tissue magnetization based on a saturation recovery image acquired with saturation time=2000 ms. T_{1a}=1650 ms is the assumed relaxation time for arterial blood, and λ=0.9 is the average partition coefficient in the brain. The constant ε=0.85×0.75 accounts for the combined effects of labeling efficiency and background suppression.

For multidelay ASL scans, a 2-compartment ASL model was applied for the i^{th} delay time PLD_i:

$$CBF(i) = 6000 \cdot \frac{e^{ATT/T_{1a}}}{2\varepsilon T_{1a}\left(e^{-\frac{\max(PLD_i - ATT, 0)}{T_{1t}}} - e^{-\frac{\max(PLD_i + LD - ATT, 0)}{T_{1t}}}\right)} \cdot \lambda \cdot \frac{M_i}{M_0} \quad (2)$$

where T_{1t}=1200 ms is the assumed relaxation for tissue. The ATT were measured using a weighted delay method and look-up table as described in Dai et al.[17] Based on the theoretical ASL signal at each PLD_i, the CBF maps from each delay time were combined through a weighted average.

Statistical Comparisons of Relative CBF

Linear registration was performed to align the ASL and PET scans to each subject's T_1-weighted MRI, followed by nonlinear registration to the Montreal Neurological Institute brain template with Advanced Normalization Tools software. Regional CBF values from cortical tissue were determined in 10 perfusion territories (2 anterior, 6 middle, and 2 posterior) per hemisphere, corresponding to 2 slice locations of the Alberta Stroke Programme Early Computed Tomography Score (ASPECTS).[18]

Relative CBF (rCBF) values were computed for each region through normalization to the mean CBF of the posterior territory, assuming that the posterior circulation in Moyamoya patients has sufficiently short ATTs to allow patient-specific corrections of CBF.[19] For 2 individuals with posterior disease involvement, only the unaffected posterior regions were used for normalization. The rCBF values were considered for regions mild Tmax delays (<3 seconds), moderate Tmax (between 3 and 5 seconds), and severe Tmax (>5 seconds) categorized by DSC. Differences in mean rCBF between each ASL sequence and PET were

assessed by paired Wilcoxon signed-rank tests, followed by conservative Bonferroni correction for multiple comparisons. For regions with moderate and severe Tmax delays, scatter and Bland–Altman plots were generated to compare ASL and PET.

Results

Figure 1 shows perfusion images from a 26-year-old woman with bilateral Moyamoya disease. In areas of prolonged Tmax, standard-delay ASL showed areas of underestimation and overestimation relative to the PET scan. Improved visual consistency with PET rCBF maps was observed with multiple-delay and LLLD ASL scans. Multidelay ASL also revealed elevated ATT that corresponded to areas of long Tmax.

Figure 2 shows a 31-year-old woman with severe bilateral Moyamoya disease and previous stroke in the left hemisphere. Although true perfusion deficits were identified on PET imaging in this patient, standard-delay ASL CBF maps had additional inaccuracies of reduced signal because of long ATTs. This signal loss was mitigated by multidelay ASL and was further improved visually by the LLLD ASL acquisition. In 2 such patients with regions of severely long delays (average Tmax > 8 seconds), all ASL sequences underestimated CBF in affected regions relative to PET.

Across patients, the largest discrepancies between ASL and PET were observed in areas commonly affected by Moyamoya pathology, such as the anterior cerebral artery and middle cerebral artery territories. The disease status of each region was classified as mild (n=181), moderate (n=56), or severe (n=33) based on Tmax delay. Across the regions with mild delays, there was no difference in rCBF between any of the 3 ASL scans compared with PET (Figure 3). Standard-delay ASL measured lower rCBF that was 73% of the PET values in regions with moderate delays (corrected $P<0.001$); and 66% of the PET values in regions of severe delays (corrected $P<0.001$). Multidelay ASL measured ATTs of 1180±371 ms in regions with mild delays, 1550±370 ms in regions with moderate delays, and 1770±340 ms in regions with severe delays ($P<0.02$; 1-way ANOVA). Through correcting for ATT, multidelay acquisition improved rCBF estimation up to 83% of the PET values in areas of moderate delays but still underestimated rCBF in areas of severe delays (corrected $P=0.02$). No difference was detected between LLLD ASL and PET rCBF values, even in the presence of moderate or severe delays.

The rCBF values from all 3 ASL acquisitions significantly correlated with PET in regions with moderate Tmax (Figure 4A). Standard-delay and multidelay ASL scans provided 16% and 8% underestimation bias, respectively, relative to PET while LLLD measurements provided minimal bias on the Bland–Altman plots. Similar observations were made in regions with severe Tmax delays (Figure 4B). Although all ASL scans correlated with PET, standard-delay and multidelay ASL scans provided 16% and 14% underestimation bias. LLLD scans had the strongest correlation with PET, as well as minimal bias (1%) relative to PET.

Discussion

This study evaluated the accuracy of several ASL MRI acquisitions to measure cerebral perfusion in patients with Moyamoya disease compared with reference [^{15}O]-water PET scans acquired simultaneously on a hybrid system. Major findings include:

1. Standard-delay ASL acquisitions with PLD of 2 seconds led to dramatic underestimation of rCBF in anterior and middle cerebral artery perfusion territories with moderate and long transit delays in patients;
2. Multidelay ASL scans improved the correlation with PET through direct consideration of ATT and a 2-compartment model but still resulted in noticeable rCBF underestimation for long transit delays; and
3. LLLD ASL acquisitions with LD of 3 seconds and PLD of 4 seconds, which was comparable to Tmax delays measured by DSC, led to the strongest CBF correlation with PET scans in cases of long transit delays.

Changes in CBF and CVR are ubiquitous in clinical Moyamoya disease, requiring monitoring throughout the patient's life. For example, accurate measurement of perfusion is critical to assess CVR, which is used clinically for initial surgical intervention and to assess the success of surgery. Although in some patient populations (eg, acute stroke), quantification may be less critical because of the focal nature of the disease; in Moyamoya disease, often both hemispheres are affected, CBF and CVR changes are less easily appreciated without quantification, and global changes are also relevant. Our results suggest that while standard-delay ASL scans are not suitable for this purpose, multidelay and LLLD scans (which are relatively untested) are appropriate imaging approaches to assess CBF in these patient cohorts. Because of its noninvasive nature and reliability compared with PET, baseline ASL scans with multiple PLDs and a long PLD can be incorporated into the MRI evaluation both before and after surgery to understand the effects of intervention. These ASL scans can also be repeated before and after a cerebrovascular challenge to assess CVR.

The novel use of simultaneous PET/MRI here allowed us to image the same brain perfusion state by both modalities, removing physiological variability that can occur between different scan sessions. A recent review of studies that compared [^{15}O]-water PET and ASL in different sessions showed stronger correlations between PET and MRI if the scans were spaced closely in time,[20] suggesting that careful control of physiology is critical for CBF validation. Because PET and ASL scans were performed simultaneously, this study achieved rCBF correlations as high as R^2=0.78 even in areas of severe disease, which are among the strongest correlations that have been reported.[20]

Previous comparisons of standard ASL sequences (PLD of ≤2 seconds) with nuclear imaging by [^{123}I]-IMP SPECT[21] ([^{123}I]-iodoamphetamine single-photon emission computed tomography) and [^{15}O]-PET[22] demonstrated clear underestimation of CBF by ASL in areas of Moyamoya disease. These regions have long transit delays relative to the PLD, leading to artificially low ASL signal that is a known confounder in highly collateralized brain regions.[13] More recently, Hara et al[23] observed that ASL with a single PLD of 2.5 seconds, which is similar to our standard PLD, outperformed ASL with a shorter PLD of 1.5 seconds in areas

of Moyamoya disease (Tmax > 6 seconds). However, only a modest relationship (R^2=0.25) between PET and ASL CBF was observed,[23] with persistent quantification bias by ASL compared with PET. ASL scans with PLD of 2 seconds have also shown local CBF hyper-intensities that likely correspond to collateral flow with long transit times,[24] and we observed similar hyperintense, intravascular signal in our standard-delay ASL scans (Figure 1).

ASL imaging with multiple PLDs and a 2-compartment model has been proposed to mitigate the effect of long ATTs. Previous work found that multidelay ASL more strongly correlated with computed tomographic perfusion than single-delay ASL (PLD of 2 seconds) in Moyamoya patients.[25] Two-compartment modeling of multidelay ASL[26] has shown 27% longer ATT's in the affected side compared with the contralateral side, similar to the 31% ATT elevation we observed in regions with moderate Tmax. Tsujikawa et al[26] also demonstrated a strong correlation between PET and multidelay ASL CBF (R^2=0.67), which was similar to our correlations in Figure 4A. However, the longest PLD used in past multidelay ASL implementations was 3 seconds[25,26] or as short as 1.5 seconds.[27] Although ATT measured by ASL and Tmax measured by DSC are not necessarily the same, the PLD range that we used may be suboptimal because the PLDs are shorter than the Tmax values in many patients.[12]

Our findings suggest that an optimal ASL protocol with longer PLD is necessary for accurate cortical CBF assessment in Moyamoya patients. Based on catheter angiography, these patients have arterial circulation times as long as 3.25 seconds,[28] motivating the use of longer PLDs to allow tagged blood to reach the capillaries. In this study, LLLD scans with PLD of 4 seconds showed the strongest correlation and the least bias of rCBF values compared with PET in areas of severe transit delays. The main disadvantage of LLLD scans, however, is the decay of ASL signal during the longer PLD before image acquisition, leading to challenges with signal-to-noise ratio. For instance, using a PLD of 4 seconds and assuming a T_{1a} of 1.65 seconds, ≈90% of labeled signal will be lost because of T1 recovery by the time of imaging. To achieve adequate signal-to-noise ratio within 5 minutes, we increased the LD and reduced the in-plane spatial resolution of the images. Even so, the LLLD ASL images had lower signal-to-noise ratio than the other ASL scans, as evidenced by higher background noise in Figures 1 and 2.

Although this study focused on cortical tissues, CBF values in the deep gray matter were noticeably reduced in LLLD ASL scans. This observation may reflect earlier blood arrival combined with faster T_1 relaxation in the tissue compared with the blood, which leads to underestimation of both ATT and CBF in early-arrival regions at longer PLDs.[17] It may also help explain why LLLD ASL did not perform as well as multidelay ASL in cases of moderate Tmax. The large range of expected ATT variations across brain regions and because of disease make it challenging to identify a single, optimal delay time for ASL in patients. Thus, comprehensive CBF assessment in Moyamoya disease may require multiple PLDs with an extended PLD range (between 0.3 and 4 seconds or longer) and use of time-efficient encoding strategies[29] to achieve clinical scan times.

As a limitation, this work did not directly measure rCBF by DSC, which is the most commonly used MRI perfusion method in Moyamoya disease. Goetti et al[13] performed 2 studies to compare single-delay ASL to DSC and to [^{15}O]-water PET,[22] respectively, on a similar cohort of young Moyamoya patients. For qualitative perfusion assessment, single-delay ASL showed similar relationships to DSC (ρ=0.77) and to PET (ρ=0.77). More recently, Hara et al[23] studied ASL, PET, and DSC in the same cohort and showed that differences between ASL scans acquired at different PLD times were predictive of DSC timing parameters, such as Tmax. Unlike DSC, however, ASL uses the same diffusible tracer (water) as PET, and we, therefore, expect optimized, multidelay ASL scans to outperform DSC when compared with PET in future studies.

Regional analysis in this study used regions of interest (ROIs) based on the ASPECTS scoring system because it is well established for evaluation of cerebral ischemia and delineates cortical perfusion territories that are relevant to assessment of cerebrovascular disease. In addition, one important clinical goal of CBF imaging in Moyamoya disease at our institution is the measurement of CVR, and our ROIs with a mean volume of 45 cm^3 are typically the smallest size in which such assessments can be reliably performed. However, this size of ROI may not be appropriate for regional comparisons of focal CBF lesions. Alternative analyses could use smaller ROIs or even voxel-wise analysis to improve the scale of the correlations. In this work, our Moyamoya patients had relatively preserved baseline perfusion because of Moyamoya collateral networks, and regional deficits typically occurred in areas of previous infarct. These more local PET hypointensities commonly corresponded to low ASL signal within that ROI, driving the CBF dynamic range of Figure 4; we would anticipate even stronger correlations with finer ROI scales. The correlations presented here, despite the large ROI volume, are nonetheless relevant to other cerebrovascular conditions, including ischemic stroke, which have large lesion volumes (median of ≈102 cm^3 across gray matter).[30]

Another limitation of this study is the lack of absolute CBF quantification, which would allow serial follow-up of Moyamoya disease and assessment of cerebrovascular reactivity. To minimize patient discomfort, we did not collect arterial blood samples, which prevents kinetic modeling of absolute CBF from the PET data. Instead, we created rCBF maps from the first 2 minutes of PET counts after the [^{15}O]-water injection; similar static PET images have been shown to accurately represent CBF if the first 40 seconds after the injection are included.[31] Future CBF comparisons will focus on quantitative evaluations between ASL and PET through use of image-based input functions for CBF quantification.[32] In addition, because atlas-based magnetic resonance attenuation correction slightly underestimates PET tracer uptake,[15] alternative attenuation correction methods based on zero-echo time MRI may improve the accuracy of absolute PET CBF values.[33]

Once these quantification issues are addressed, simultaneous PET/MRI provides an ideal strategy to validate advanced ASL techniques, such as velocity-selective ASL,[34] that hold promise in challenging cerebrovascular cases. Furthermore, oxygen extraction fraction and the cerebral metabolic rate of oxygen are also critical biomarkers to characterize hemodynamic impairment in Moyamoya disease[6] and evaluate its treatment. As novel MRI methods to assess oxygen extraction fraction and cerebral metabolic rate of oxygen gain

traction,[35] the PET/MRI hybrid modality offers careful control of cerebral physiology to validate these new measurements against the triple [^{15}O]-PET reference standard.[36]

Conclusions

We compared CBF measurements with multiple ASL techniques against the PET reference standard in patients with Moyamoya disease under simultaneous conditions. LLLD ASL showed the least bias in rCBF values compared with PET, enabling reliable CBF assessment even in areas of severe Tmax delay. We demonstrated that extremely long PLD's are required for ASL studies in cerebrovascular disease, and any multiple-delay time acquisitions should include a wide range of post-label delays (eg, between 0.3 and 4 seconds).

Acknowledgments

We thank Jarrett Rosenberg for insightful discussions regarding statistical approach. We also thank Jezica Tagle and Teresa Bell-Stephens for support in patient recruitment.

Sources of Funding

This study was funded by General Electric Healthcare. Audrey Fan is supported by the Stanford Neurosciences Institute Interdisciplinary Scholar Award.

Disclosures

Dr Khalighi is employed by General Electric Healthcare, and Dr Zaharchuk receives funding support from General Electric Healthcare. The other authors report no conflicts.

References

1. Suzuki J, Takaku A. Cerebrovascular "moyamoya" disease. Disease showing abnormal net-like vessels in base of brain. Arch Neurol. 1969;20:288–299. [PubMed: 5775283]
2. Kobayashi E, Saeki N, Oishi H, Hirai S, Yamaura A. Long-term natural history of hemorrhagic moyamoya disease in 42 patients. J Neurosurg. 2000;93:976–980. doi: 10.3171/jns.2000.93.6.0976. [PubMed: 11117870]
3. Yamada M, Fujii K, Fukui M. [Clinical features and outcomes in patients with asymptomatic moyamoya disease–from the results of nation-wide questionnaire survey]. No Shinkei Geka. 2005;33:337–342. [PubMed: 15830539]
4. Nariai T, Matsushima Y, Imae S, Tanaka Y, Ishii K, Senda M, et al. Severe haemodynamic stress in selected subtypes of patients with moyamoya disease: a positron emission tomography study. J Neurol Neurosurg Psychiatry. 2005;76:663–669. doi: 10.1136/jnnp.2003.025049. [PubMed: 15834024]
5. Ikezaki K, Matsushima T, Kuwabara Y, Suzuki SO, Nomura T, Fukui M. Cerebral circulation and oxygen metabolism in childhood moyamoya disease: a perioperative positron emission tomography study. J Neurosurg. 1994;81:843–850. doi: 10.3171/jns.1994.81.6.0843. [PubMed: 7965114]
6. Kuwabara Y, Ichiya Y, Sasaki M, Yoshida T, Masuda K, Ikezaki K, et al. Cerebral hemodynamics and metabolism in moyamoya disease–a positron emission tomography study. Clin Neurol Neurosurg. 1997;99 (suppl 2):S74–S78. [PubMed: 9409411]
7. Kim SK, Wang KC, Oh CW, Kim IO, Lee DS, Song IC, et al. Evaluation of cerebral hemodynamics with perfusion MRI in childhood moyamoya disease. Pediatr Neurosurg. 2003;38:68–75. doi: 68050. [PubMed: 12566838]
8. Calamante F, Ganesan V, Kirkham FJ, Jan W, Chong WK, Gadian DG, et al. MR perfusion imaging in Moyamoya syndrome: potential implications for clinical evaluation of occlusive cerebrovascular disease. Stroke. 2001;32:2810–2816. [PubMed: 11739978]

9. Yun TJ, Cheon JE, Na DG, Kim WS, Kim IO, Chang KH, et al. Childhood moyamoya disease: quantitative evaluation of perfusion MR imaging–correlation with clinical outcome after revascularization surgery. Radiology. 2009;251:216–223. doi: 10.1148/radiol.2511080654. [PubMed: 19332853]
10. Detre JA, Alsop DC. Perfusion magnetic resonance imaging with continuous arterial spin labeling: methods and clinical applications in the central nervous system. Eur J Radiol. 1999;30:115–124. [PubMed: 10401592]
11. Alsop DC, Detre JA, Golay X, Günther M, Hendrikse J, Hernandez-Garcia L, et al. Recommended implementation of arterial spin-labeled perfusion MRI for clinical applications: a consensus of the ISMRM perfusion study group and the European consortium for ASL in dementia. Magn Reson Med. 2015;73:102–116. doi: 10.1002/mrm.25197. [PubMed: 24715426]
12. Yun TJ, Sohn CH, Han MH, Kang HS, Kim JE, Yoon BW, et al. Effect of delayed transit time on arterial spin labeling: correlation with dynamic susceptibility contrast perfusion magnetic resonance in moyamoya disease. Invest Radiol. 2013;48:795–802. doi: 10.1097/RLI.0b013e3182981137. [PubMed: 23764569]
13. Goetti R, O'Gorman R, Khan N, Kellenberger CJ, Scheer I. Arterial spin labelling MRI for assessment of cerebral perfusion in children with moyamoya disease: comparison with dynamic susceptibility contrast MRI. Neuroradiology. 2013;55:639–647. doi: 10.1007/s00234-013-1155-8. [PubMed: 23404242]
14. Yoneda K, Harada M, Morita N, Nishitani H, Uno M, Matsuda T. Comparison of FAIR technique with different inversion times and post contrast dynamic perfusion MRI in chronic occlusive cerebrovascular disease. Magn Reson Imaging. 2003;21:701–705. [PubMed: 14559333]
15. Sekine T, Buck A, Delso G, Ter Voert EE, Huellner M, Veit-Haibach P, et al. Evaluation of atlas-based attenuation correction for integrated PET/MR in human brain: application of a head atlas and comparison to true CT-based attenuation correction. J Nucl Med. 2016;57:215–220. doi: 10.2967/jnumed.115.159228. [PubMed: 26493207]
16. Straka M, Albers GW, Bammer R. Real-time diffusion-perfusion mismatch analysis in acute stroke. J Magn Reson Imaging. 2010;32:1024–1037. doi: 10.1002/jmri.22338. [PubMed: 21031505]
17. Dai W, Robson PM, Shankaranarayanan A, Alsop DC. Reduced resolution transit delay prescan for quantitative continuous arterial spin labeling perfusion imaging. Magn Reson Med. 2012;67:1252–1265. doi: 10.1002/mrm.23103. [PubMed: 22084006]
18. Kim JJ, Fischbein NJ, Lu Y, Pham D, Dillon WP. Regional angiographic grading system for collateral flow: correlation with cerebral infarction in patients with middle cerebral artery occlusion. Stroke. 2004;35:1340–1344. doi: 10.1161/01.STR.0000126043.83777.3a. [PubMed: 15087564]
19. Zaharchuk G, Straka M, Marks MP, Albers GW, Moseley ME, Bammer R. Combined arterial spin label and dynamic susceptibility contrast measurement of cerebral blood flow. Magn Reson Med. 2010;63:1548–1556. doi: 10.1002/mrm.22329. [PubMed: 20512858]
20. Fan AP, Jahanian H, Holdsworth SJ, Zaharchuk G. Comparison of cerebral blood flow measurement with [15O]-water positron emission tomography and arterial spin labeling magnetic resonance imaging: a systematic review. J Cereb Blood Flow Metab. 2016;36:842–861. doi: 10.1177/0271678X16636393. [PubMed: 26945019]
21. Noguchi T, Kawashima M, Irie H, Ootsuka T, Nishihara M, Matsushima T, et al. Arterial spin-labeling MR imaging in moyamoya disease compared with SPECT imaging. Eur J Radiol. 2011;80:e557–e562. doi: 10.1016/j.ejrad.2011.01.016. [PubMed: 21315533]
22. Goetti R, Warnock G, Kuhn FP, Guggenberger R, O'Gorman R, Buck A, et al. Quantitative cerebral perfusion imaging in children and young adults with Moyamoya disease: comparison of arterial spin-labeling-MRI and H(2)[(15)O]-PET. AJNR Am J Neuroradiol. 2014;35:1022–1028. doi: 10.3174/ajnr.A3799. [PubMed: 24335546]
23. Hara S, Tanaka Y, Ueda Y, Hayashi S, Inaji M, Ishiwata K, et al. Noninvasive evaluation of CBF and perfusion delay of Moyamoya disease using arterial spin-labeling MRI with multiple postlabeling delays: comparison with (15)O-Gas PET and DSC-MRI. AJNR Am J Neuroradiol. 2017;38:696–702. doi: 10.3174/ajnr.A5068. [PubMed: 28209582]

24. Zaharchuk G, Do HM, Marks MP, Rosenberg J, Moseley ME, Steinberg GK. Arterial spin-labeling MRI can identify the presence and intensity of collateral perfusion in patients with moyamoya disease. Stroke. 2011;42:2485–2491. doi: 10.1161/STROKEAHA.111.616466. [PubMed: 21799169]
25. Wang R, Yu S, Alger JR, Zuo Z, Chen J, Wang R, et al. Multi-delay arterial spin labeling perfusion MRI in moyamoya disease–comparison with CT perfusion imaging. Eur Radiol. 2014;24:1135–1144. doi: 10.1007/s00330-014-3098-9. [PubMed: 24557051]
26. Tsujikawa T, Kimura H, Matsuda T, Fujiwara Y, Isozaki M, Kikuta K, et al. Arterial transit time mapping obtained by pulsed continuous 3D ASL imaging with multiple post-label delay acquisitions: comparative study with PET-CBF in patients with chronic occlusive cerebrovascular disease. PLoS One. 2016;11:e0156005. doi: 10.1371/journal.pone.0156005. [PubMed: 27275779]
27. Saida T, Masumoto T, Nakai Y, Shiigai M, Matsumura A, Minami M. Moyamoya disease: evaluation of postoperative revascularization using multiphase selective arterial spin labeling MRI. J Comput Assist Tomogr. 2012;36:143–149. doi: 10.1097/RCT.0b013e31824150dd. [PubMed: 22261785]
28. Donahue MJ, Ayad M, Moore R, van Osch M, Singer R, Clemmons P, et al. Relationships between hypercarbic reactivity, cerebral blood flow, and arterial circulation times in patients with moyamoya disease. J Magn Reson Imaging. 2013;38:1129–1139. doi: 10.1002/jmri.24070. [PubMed: 23440909]
29. Dai W, Shankaranarayanan A, Alsop DC. Volumetric measurement of perfusion and arterial transit delay using Hadamard encoded continuous arterial spin labeling. Magn Reson Med. 2013;69:1014–1022. doi: 10.1002/mrm.24335. [PubMed: 22618894]
30. Sperber C, Karnath HO. Topography of acute stroke in a sample of 439 right brain damaged patients. Neuroimage Clin. 2016;10:124–128. doi: 10.1016/j.nicl.2015.11.012. [PubMed: 26759787]
31. Koeppe RA, Hutchins GD, Rothley JM, Hichwa RD. Examination of assumptions for local cerebral blood flow studies in PET. J Nucl Med. 1987;28:1695–1703. [PubMed: 3499491]
32. Khalighi MM, Deller TW, Fan AP, Gulaka PK, Shen B, Singh P, et al. Image-derived input function estimation on a TOF-enabled PET/MR for cerebral blood flow mapping. J Cereb Blood Flow Metab. 2017. doi: 10.1177/0271678X17691784.
33. Sekine T, Ter Voert EE, Warnock G, Buck A, Huellner M, Veit-Haibach P, et al. Clinical evaluation of zero-echo-time attenuation correction for brain 18F-FDG PET/MRI: comparison with atlas attenuation correction. J Nucl Med. 2016;57:1927–1932. doi: 10.2967/jnumed.116.175398. [PubMed: 27339875]
34. Qiu D, Straka M, Zun Z, Bammer R, Moseley ME, Zaharchuk G. CBF measurements using multidelay pseudocontinuous and velocity-selective arterial spin labeling in patients with long arterial transit delays: comparison with xenon CT CBF. J Magn Reson Imaging. 2012;36:110–119. doi: 10.1002/jmri.23613. [PubMed: 22359345]
35. Christen T, Bolar DS, Zaharchuk G. Imaging brain oxygenation with MRI using blood oxygenation approaches: methods, validation, and clinical applications. AJNR Am J Neuroradiol. 2013;34:1113–1123. doi: 10.3174/ajnr.A3070. [PubMed: 22859287]
36. Mintun MA, Raichle ME, Martin WR, Herscovitch P. Brain oxygen utilization measured with O-15 radiotracers and positron emission tomography. J Nucl Med. 1984;25:177–187. [PubMed: 6610032]

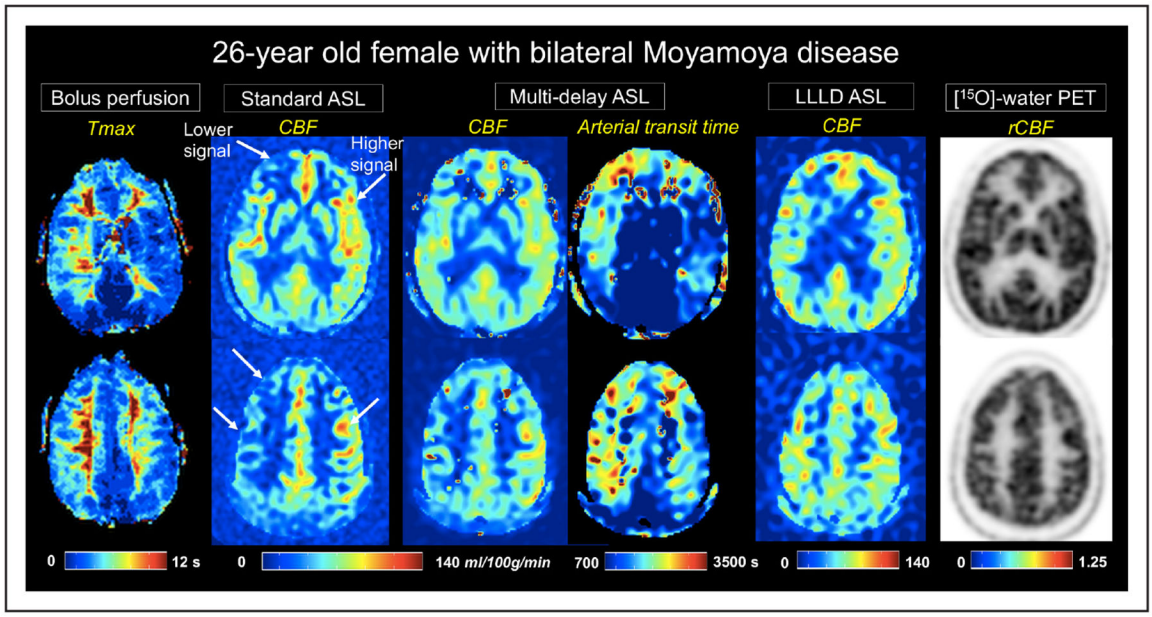

Figure 1.

A 26-year-old female patient with bilateral Moyamoya disease. Time-to-maximum (Tmax) images from dynamic susceptibility contrast MRI are shown on the leftmost panel. Cerebral blood flow (CBF) maps (mL/100 g per minute) from each of the 3 arterial spin labeling (ASL) acquisitions are depicted at 2 slice locations, as well as arterial transit time from multidelay ASL. Arrows indicate areas of lower and higher signal on standard single-delay ASL relative to the [^{15}O]-water positron emission tomography (PET) reference (far right). Improved cortical CBF measurement compared with PET is seen on multidelay and long-label long-delay (LLLD) ASL scans. rCBF indicates relative CBF.

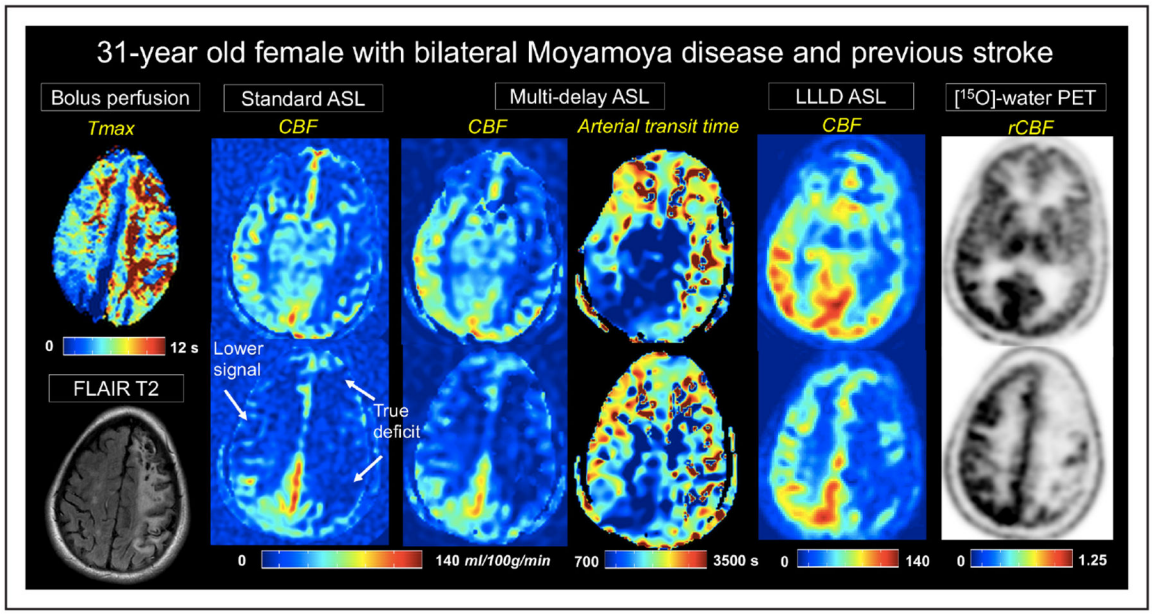

Figure 2.

A 31-year-old women with severe, bilateral Moyamoya disease and a previous stroke on left hemisphere. Time-to-maximum (Tmax) images from dynamic susceptibility contrast are shown on the leftmost panel. Cerebral blood flow (CBF) maps (mL/100 g per minute) from each of the 3 arterial spin labeling (ASL) acquisitions are depicted at 2 slice locations, as well as arterial transit time from multidelay ASL. Signal loss on standard single-delay ASL relative to positron emission tomography (PET), because of long arterial transit times, are evident in the right hemisphere. This signal loss is partially recovered in multidelay ASL, and more fully recovered with long-label long-delay (LLLD) ASL. LLLD ASL allows distinction between nonperfused tissue from the stroke and perfused tissue with extremely long Tmax. rCBF indicates relative CBF.

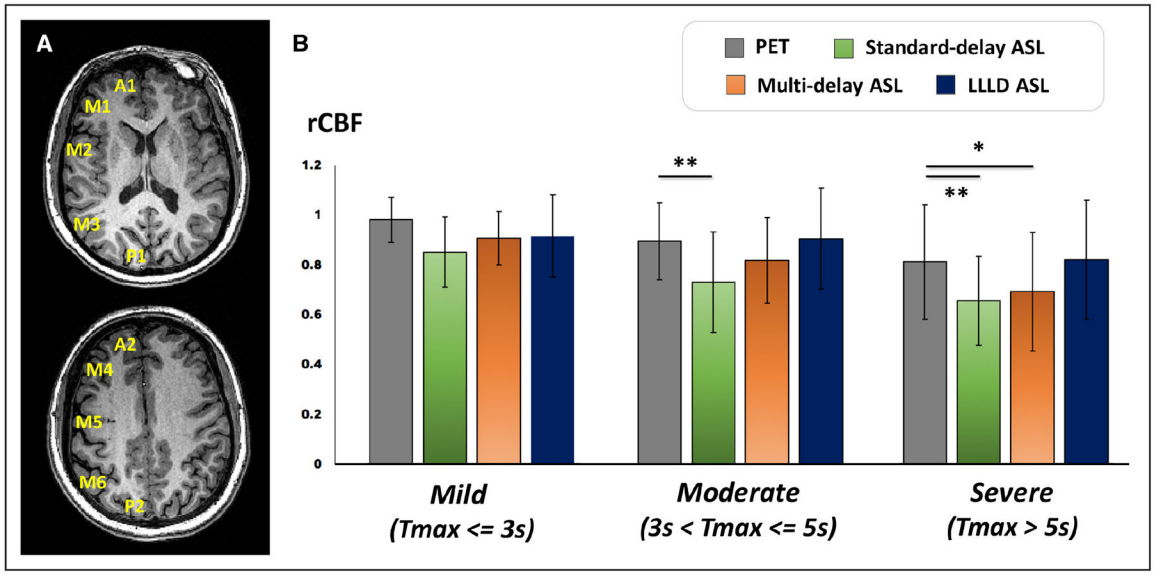

Figure 3.

Relative CBF (rCBF) averaged across 15 patients with Moyamoya disease in different perfusion territories based on the Alberta Stroke Programme Early Computed Tomography scoring system. **A**, Cortical regions include A, anterior circulation; P, posterior circulation; M1 and M4, anterior middle cerebral artery (MCA) territory; M2 and M5, lateral MCA territory; M3 and M6 posterior MCA territory. **B**, Positron emission tomography (PET) and arterial spin labeling (ASL) rCBF in regions of different time-to-maximum (Tmax) delays as measured by dynamic susceptibility contrast. Mean and SD of rCBF are shown for 181 regions with mild Tmax, 56 regions with moderate Tmax, and 33 regions with severe Tmax delays. Asterisks indicate significant difference in mean rCBF from PET reference standard by Wilcoxon signed-rank test after correction for multiple comparisons. LLLD indicates long-label long-delay.

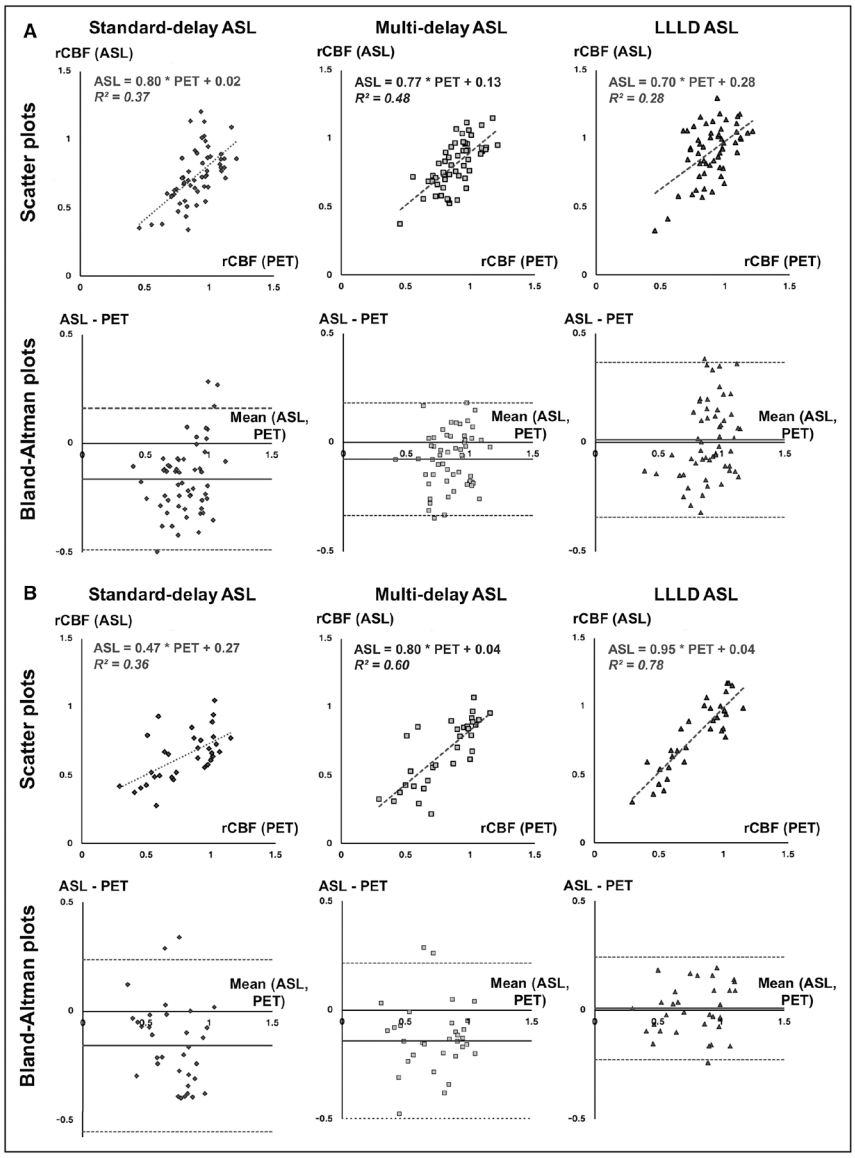

Figure 4.

Linear regression analysis to evaluate the agreement between standard, multidelay, and long-label long-delay (LLLD) arterial spin labeling (ASL) with the positron emission tomography (PET) reference standard. Scatter plots of relative cerebral blood flow (rCBF) with linear fits and Bland–Altman plots (mean vs difference) are shown for (**A**) regions of moderate time-to-maximum (Tmax) delays (n=56) and (**B**) regions of severe Tmax delays (n=33) identified on dynamic susceptibility contrast MRI.

Table 1.

Patient Demographic and Clinical Information

Patient	Age, y/Sex	Bilateral/Unilateral	Posterior Involvement	Clinical History
1	34/M	Bilateral supraclinoid ICA occlusion	No	Daily occipital headaches.
2	31/F	Left ICA occlusion	No	Sudden-onset aphasia and loss of strength on right side. Previous stroke in left MCA territory.
3	46/F	Narrowing of supraclinoid ICA, right M1, right A1	No	History of morning glory syndrome, premature ventricular contractions, and endometriosis.
4	46/M	Right ICA stenosis, right MCA occlusion	No	Right body numbness, difficulty swallowing, and unsteady gait.
5	34/F	Right M1 occlusion, left M1 stenosis	No	Right-sided weakness, right facial droop, slurred speech, tingling in left hand and face, headaches. Previous left parietal stroke.
6	49/F	Right M1 occlusion, left ICA stenosis	No	Aphasia with slurred speech, left facial droop, confusion.
7	16/F	Bilateral ICA stenosis, M1 occlusion	Yes	Sickle cell disorder, history of malaria, speech arrest, right-sided weakness, and numbness in fingertips.
8	26/F	Bilateral stenosis of supraclinoid ICA	No	Dizziness, left hand weakness, tingling in left arm and face, numbness. Previous left-sided stroke.
9	45/F	Left ICA occlusion, stenosis of right M1 and right A1.	No	History of Hashimoto disease. Right body weakness, speech impairment, left-sided weakness, and severe headache. Previous left frontal stroke.
10	51/F	Bilateral stenosis of M1.	No	Bilateral numbness, weakness, loss of speech, and headaches. Recurrent confusion after 2 prior bypasses.
11	32/F	Bilateral ICA occlusion	No	Bilateral EC-IC bypass at age 10 y after strokes. Migraines, seizures, and visual changes.
12	25/F	Occlusion of left A1, right supraclinoid ICA, stenosis of left supraclinoid ICA	No	Severe headache, right facial and body numbness, central tremors, garbled speech, and memory issues. Right frontal stroke.
13	52/M	Right ICA stenosis, right M1 occlusion	No	Headaches, numbness in left hand, loss of visual field on left. Old watershed strokes.
14	44/M	Occlusion of right supraclinoid ICA, stenosis of left supraclinoid ICA	Yes	Slurred speech with drooling, transient coordination issues. Bilateral watershed infarcts, greater on the right.
15	25/F	Bilateral MCA occlusion	No	Headaches, transient right body, and left foot weakness. Bilateral watershed infarcts.

EC-IC indicates extracranial to intracranial; F, female; ICA, internal carotid artery; M, male; and MCA, middle cerebral artery.

Table 2.

ASL MRI Acquisition Parameters

	Standard ASL	Multidelay ASL	Long-Label Long-Delay
Repetition time, ms	4852	6489	8489
Echo time, ms	10.7	10.7	10.7
Label duration, ms	1500	2000	3000
Post-label delay, ms	2025	5 equally spaced between 700 and 3000	4000
In-plane resolution, mm	3.7×3.7	5.8×5.8	5.8×5.8
Slice thickness, mm	4.0	4.0	4.0
Spiral # arms	8	4	4
Points/arm	512	512	512
# Averages	3	1	4
Bandwidth, kHz	62.5	62.5	62.5
Scan duration, min	4:42	4:46	5:06

ASL indicates arterial spin labeling.